Monte Carlo Results for a Linear Polymer Confined to a Harmonic Potential Well

J. James,† G. C. Barker,*,‡ and M. Silbert§

Met 011, Metereological Office, London Road, Bracknell Berkshire, U.K., Theory and Computational Science Group, AFRC Institute of Food Research, Colney Lane, Norwich NR4 7UA, U.K., and Departamento de Fisica Teorica, Facultad de Cienicas, Universidad de Valladolid, 47011 Valladolid, Spain

Received September 28, 1990; Revised Manuscript Received December 26, 1990

ABSTRACT: The configurational and thermodynamic properties of a single polymer chain have been studied by Monte Carlo simulation methods. The model consists of a bead-spring polymer confined in a variable harmonic potential well. The results for the mean-square radius of gyration were found to be in good qualitative agreement with those obtained from comparable lattice models. A continuous transition from three- to two-dimensional behavior is observed. The expectation values, describing the interaction of the polymer with the external potential, approach limits, independent of the external potential, as the chain is compressed into a monolayer.

1. Introduction

Food constituents such as native or modified proteins, lipids, and added emulsifiers or stabilizers have the ability to congregate at air/water, oil/water, and solid/water interfaces. This illustrates one of the many reasons for the continuing interest in the study of flexible macromolecules at interfaces. Thus polymers confined to slabs and slits,[1] the interaction of polymers with penetrable surfaces,[2] and polymers trapped in porous media[3] have been studied by using many different approaches and techniques.

Given the complexity of flexible macromolecules, drastic assumptions and approximations are necessary in order to make theoretical models. The approximations aim to bring to the forefront those features and properties of the system that are the subject of the investigation. Both discrete and continuum models have been employed within theoretical and/or computational frameworks. We use a continuum, bead–spring, model[4] and a Monte Carlo computer simulation technique.[5] In the bead–spring model, all the beads interact via a repulsive, shifted, Lennard-Jones potential and nearest neighbors along the chain are linked by a quasi-harmonic potential, which allows for limited spring extensions. Rather than[1-3] present results for macromolecules that are already within a confined geometry or at an interface, we give results of simulations in which the behavior of a linear polymer changes as it is confined by a harmonic potential well, which has a variable coupling constant. In this way we model the interactions leading to the adsorption of the polymer at the interface and trace the transition from three- to two-dimensional behavior.

In section 2 we outline the Monte Carlo method and give details of the interaction potentials. Results are presented in section 3. These are subdivided into those relating to polymer shape, such as the components of the radius of gyration, and those relating to the thermodynamic properties, such as the contributions to the internal energy.

2. Monte Carlo Method

Consider a single linear polymer, which has a degree of polymerization N and which is in the limit of dynamic flexibility in a good solvent. The polymer is represented by beads connected by springs. Adjacent beads, separated by a distance r, interact through a modified harmonic potential

$$V_1(r) = -V_0 \ln (1 - (r/r_0)^2) \qquad r \leq r_0$$
$$= \infty \qquad r > r_0 \tag{2.1}$$

V_1 constrains the separation of neighboring monomers to be less than r_0 and has the form of a harmonic potential, with spring constant $2V_0/r_0^2$, at small r.

Excluded-volume effects, which act between all pairs of monomers and which are due to their finite size, are incorporated through a repulsive shifted Lennard-Jones (LJ) potential

$$V_2(r) = \xi((\sigma/r)^{12} - (\sigma/r)^6 + 1/4) \qquad r < 2^{1/6}\sigma$$
$$= 0 \qquad r > 2^{1/6}\sigma \tag{2.2}$$

where $2^{1/6}\sigma$ is the position of the minimum in the potential and ξ is 4 times the well depth. The effect of a good solvent can be modeled by omitting the attractive LJ tail, and long-range hydrodynamic effects are ignored. The total interaction potential for adjacent monomers, $V_1 + V_2$, is shown in Figure 1.

A variable compressive force, with a magnitude parametrized by k, is included by adding the anisotropic external potential

$$V_3(z) = kz^2 \tag{2.3}$$

The total configurational energy of the system is

$$V(\{r\}) = \sum_{\substack{i=1 \\ j=i+1}}^{N-1} V_1(|r_i - r_j|) + \sum_{i<j} V_2(|r_i - r_j|) + \sum_{i=1}^{N} V_3(z_i) \tag{2.4}$$

Initial polymer configurations were generated as random walks with step lengths uniformly distributed on $[0, r_0]$. For the most confining potentials the walks are chosen in the $z = 0$ plane, and therefore equilibration represents out-of-plane relaxation. Otherwise, the initial configuration was fully three-dimensional. Results are independent of these initial configurations. New configurations were generated by successive random displacements of monomers, and they were weighted by using a standard Metropolis algorithm.[5] The displacements are chosen uniformly from a trial volume $\Delta V = \Delta x \Delta y \Delta z$. In strong external potentials the monomers move out of the $z = 0$

† Metereological Office.
‡ AFRC Institute of Food Research.
§ Universidad de Valladolid. On study leave from the School of Physics, University of East Anglia, Norwich NR4 7TJ, U.K.

0024-9297/91/2224-3584$02.50/0

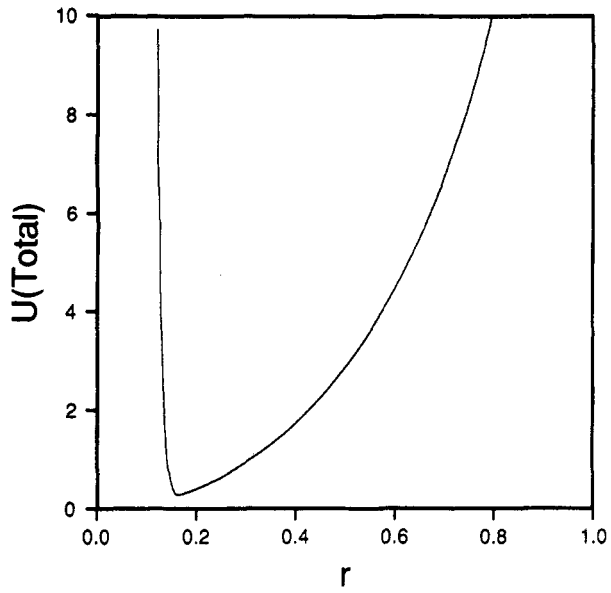

Figure 1. Total interaction potential for adjacent monomers in the bead–spring model with $V_0 = 10$ and $\sigma = 0.15$.

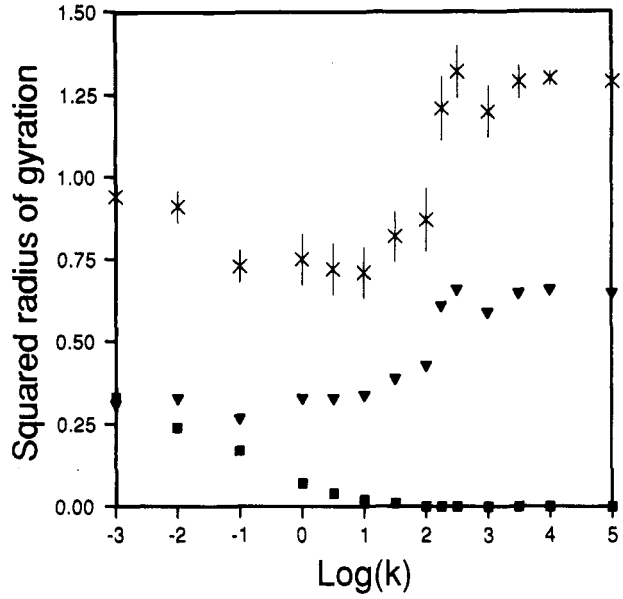

Figure 2. Mean-square radius of gyration as a function of log k for a chain with $N = 30$: (×) $\langle R_G^2 \rangle$, (▼) $\langle R_{Gz}^2 \rangle$, (■) $\langle R_{Gz}^2 \rangle$.

plane very infrequently so that, for long chains, an efficient sampling of the configuration space is achieved by reducing the trial volume anisotropically Typically, $\Delta x = \Delta y = m\Delta z = 0.1$ with $m \sim 20$. This choice maintains maximum mobility in the $z = 0$ plane but avoids serious sample attrition and therefore leads to manageable equilibration times. Suitable choice of m gives a Monte Carlo acceptance fraction of ~50% for all $\log k \leq 6$. For each simulation the total internal energy of the chain, initially, varies systematically with the number of Monte Carlo steps, but, eventually, it fluctuates randomly about a steady value. The rate of this transition and the size of the equilibrium fluctuations are a complex function of the thermodynamic variables and cannot be discussed at length here. However, by monitoring the mean internal energy, evaluated over batches of ~1000 consecutive configurations, the onset of the equilibrium phase can be established. Typically, for $N = 23$, $\sim 2 \times 10^5$ Monte Carlo steps were required for equilibration and ensemble averages were taken over a further $\sim 10^6$ consecutive configurations.

3. Results

Results are given in reduced units. In particular, lengths are given in units of r_0 and energy in units of ξ. Below we use $V_0 = 10$, $\sigma = 0.15$, and $N = 30$, unless otherwise stated. The thermal energy $k_B T = 1$.

3.1. Polymer Configurations. Figure 2 shows the variation, with $\log k$, of the mean-square radius of gyration, $\langle R_G^2 \rangle$, and the three orthogonal components $\langle R_{Gx}^2 \rangle$, $\langle R_{Gy}^2 \rangle$, and $\langle R_{Gz}^2 \rangle$, where

$$\langle R_G^2 \rangle = N^{-2} \sum_{i<j} |r_i - r_j|^2 \tag{3.1}$$

$$\langle R_{Gz}^2 \rangle = N^{-2} \sum_{i<j} |z_i - z_j|^2 \tag{3.2}$$

and

$$\langle R_{Gx}^2 \rangle = \langle R_{Gy}^2 \rangle = (\langle R_G^2 \rangle - \langle R_{Gz}^2 \rangle)/2 \tag{3.3}$$

The form of $\langle R_G^2 \rangle$ is in qualitative agreement with results of lattice simulations in which a chain is confined between hard walls (e.g., Lax et al. and Wall et al.[1]). In the regime $\log k < -3.0$, the polymer is essentially unperturbed with $\langle R_{Gx}^2 \rangle = \langle R_{Gy}^2 \rangle = \langle R_{Gz}^2 \rangle = \langle R_G^2 \rangle/3$. For $-3.0 < \log k < 1.0$, $\langle R_{Gx}^2 \rangle$ and $\langle R_{Gy}^2 \rangle$ show little increase, suggesting that the polymer increases in density rather than spreading over the xy plane. We note that a purely orientational response to confinement would leave $\langle R_G^2 \rangle$ invarient, and therefore the average transverse component of the radius of gyration should rise to compensate for a fall of $\langle R_{Gz}^2 \rangle$. This has not been observed, and therefore we conclude that the polymer has a deformational response to the applied external field. This conclusion is in contrast to those of recent lattice simulations by van Vliet and ten Brinke,[1] which use hard walls, where there is an orientational rearrangement before deformation begins. As $\log k$ increases further, the probability of nonmonolayer configurations decreases rapidly. The excluded-volume repulsion does not allow further compression without increase of the surface area in the $z = 0$ plane, so that $\langle R_{Gx}^2 \rangle$ and $\langle R_{Gy}^2 \rangle$ increase sharply. $\langle R_G^2 \rangle$ attains its two-dimensional value. Once the polymer has been compressed into a monolayer, further increase in $\log k$ only serves to reduce the magnitude of the transverse oscillations of individual monomers out of the plane. We note that previous simulation studies dealing with the collapse of single chains onto a plane, for example, Grimson[6] and Bishop and Clarke,[7] have concentrated on the behavior of tethered chains or on chains that are terminally attached to hard walls.

During compression the contour length, $\langle L \rangle = \sum_{i=1}^{N-1} |r_{i+1} - r_i|$, decreases. This indicates increased monomer/monomer interactions in the squashed regime. Figure 3 shows snapshots of polymer configurations, projected onto the xy and xz planes, for $N = 23$ and $\log k = -1.2$, 1.4, and 1.8. The degree of confinement is clearly visible.

Finally we turn to the change of the Flory exponent ν from $\nu_{3D} = 0.59$ to $\nu_{2D} = 0.75$.[5] The scaling law is such that a log–log plot of N against $\langle R_G^2 \rangle^{1/2}$ has a straight line with gradient ν. Computational constraints have restricted the values of chain length, $N < 23$, so that errors in the estimates of the Flory exponents are ~10%. This accuracy is sufficient to give a qualitative picture of the reduction of the dimensionality of the chain. We have obtained values of ν from simulations with $N = 3$, 8, 13, 18, and 23 at six values of the compressive force $\log k = 0$, 1, 1.5, 1.7, 2, and 2.8. Figure 4 gives ν as a function of $\log k$, the "crossover plot". The crossover from three- to two-dimensional behavior occurs continuously for $0.5 > \log k > 2.0$, which is in agreement with the interpretation of

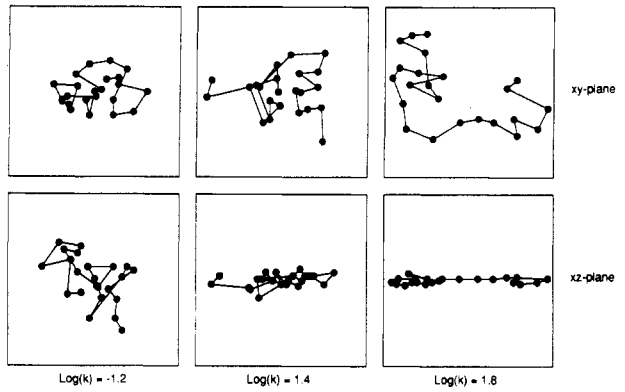

Figure 3. Example chain configurations, projected onto the xy and the xz planes, for $N = 23$ and external potentials with log $k = -1.2$, 1.4, and 1.8.

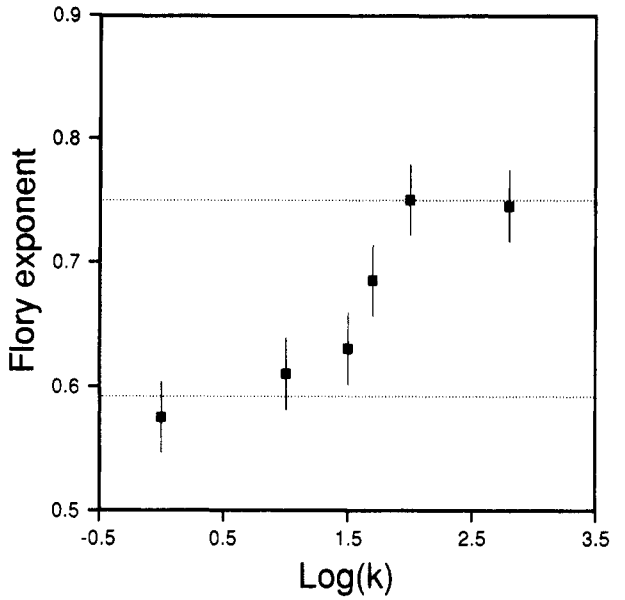

Figure 4. Crossover plot for the Flory exponent as a function of the external potential. Horizontal lines at 0.75 and 0.59 represent the theoretical values for two and three dimensions.

results given above. Since we have performed simulations of chains that have a finite length, we cannot comment on the precise form of the crossover in behavior. We note that $\nu = \nu(k)$ also depends on the particular form chosen for the confining potential, but, in the limiting cases of log $k = 0$ and log k = large, the universal results are recovered.

3.2. Thermodynamics. We consider the three components of the expectation value for the internal energy.

The expectation values of the spring potential energy, $\langle U_1 \rangle$, decreases as k increases, which is consistent with the decrease of the contour length. The excluded-volume potential energy, $\langle U_2 \rangle$, increases with k as the dimensionality is reduced. We note that $\langle U_2 \rangle = 0$ for dimensionalities greater than 4.

After the transition to two dimensions takes place, the expectation value of the external potential energy, $\langle U_3 \rangle$, tends to a constant value, A. For $N = 30$ we find $A = 15.0 k_B T$. Similar results for $N = 5$ and 15, shown in Figure 5, suggest that

$$\langle U_3 \rangle_{2D} = N k_B T/2 \qquad (3.4)$$

This result indicates that the motion of the polymer perpendicular to the xy plane can be represented by that of N independent harmonic oscillators. In this case the expectation value of the external energy is independent of k.

Finally we note that in Figure 5 $\langle U_3 \rangle$ has a maximum, at log $k \sim 2.3$, the height of which depends on N. The

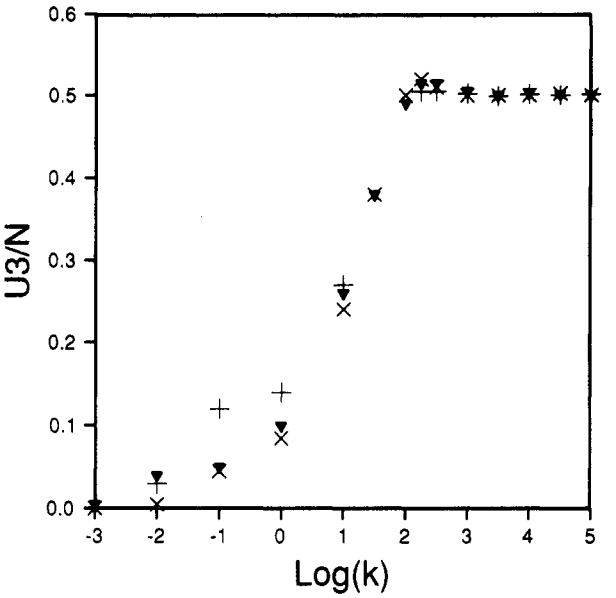

Figure 5. Expectation values of the external potential energy per monomer, $\langle U_3 \rangle / N$, as a function of log k for three different chain lengths, $N = 5$, 15, and 30 (+, ▼, ×). The maximum error decreases from 0.30 for log $k = -3$ to 0.01 for log $k > 2$.

position of this maximum coincides with the large increase in $\langle R_G^2 \rangle$ which is the point where the monomer/monomer interactions prevent further compression without a corresponding increase in the transverse components of $\langle R_G^2 \rangle$.

4. Discussion

We have performed Monte Carlo simulations of a bead–spring polymer in a continuous soft potential well. The components of the radius of gyration and the contributions to the internal energy were measured. They provide a clear picture of the changing shape of the polymer coil and illustrate the transition from three- to two-dimensional behavior. There is no evidence for an orientational ordering prior to the polymer shape deformations. There is a continuous decrease of the contour length throughout this transition. The contribution of the external potential to the internal energy of the polymer approaches a limit, which indicates restricted out-of-plane motions.

Acknowledgment. We thank M. J. Grimson for useful discussions. J. J. is grateful to the Northampton education authority for the provision of a studentship tenable at the University of East Anglia where this work was carried out. M.S. gratefully acknowledges the DGICYT of Spain for the provision of a visiting fellowship.

References and Notes

(1) Wall, F. T.; Mandel, F.; Chin, J. C. *J. Chem. Phys.* **1976**, *65*, 2231. Wall, F. T.; Seitz, W. A.; Chin, J. C. *J. Chem. Phys.* **1977**, *67*, 434. Middlemiss, K. M.; Torrie, G. M.; Whittington, S. G. *J. Chem. Phys.* **1977**, *66*, 3227. Bar, R.; Brenda, C.; Lax, M. *J. Chem. Phys.* **1980**, *72*, 2702. Lax, M.; Bar, R.; Brenda, C. *J. Chem. Phys.* **1981**, *75*, 460. Wang, Z.-G.; Nemirovsky, A. M.; Freed, K. F. *J. Chem. Phys.* **1986**, *85*, 3068. Van Vliet, J. H.; ten Brinke, G. *J. Chem. Phys.* **1990**, *93*, 1436.

(2) Hammersley, J. M.; Torrie, G. M.; Whittington, S. G. *J. Phys. A.* **1982**, *15*, 539. Kosmas, M. K. *J. Phys. A.* **1983**, *18*, 539. Ishinabe, T. *J. Chem. Phys.* **1983**, *80*, 1318. Kremer, K. *J. Chem. Phys.* **1985**, *83*, 5882.

(3) Daoud, M.; de Gennes, P.-G. *J. Phys.* **1977**, *38*, 85. Baumgartner, A.; Muthukumar, M. *J. Chem. Phys.* **1987**, *87*, 3082.

(4) Bishop, M.; Kalos, M. H.; Frisch, H. L. *J. Chem. Phys.* **1979**, *70*, 1299.

(5) *Applications of the Monte Carlo Method in Statistical Physics*; Binder, K., Ed.; Springer-Verlag: Berlin, 1984.

(6) Grimson, M. J. To be published.

(7) Bishop, M.; Clarke, J. H. R. *J. Chem. Phys.* **1990**, *93*, 1455.